

# Deep Learning-Based Method for Anatomical Subsite-wise Evaluation of Single Cell Necrosis and Vacuolation of Neuron/Nerve Fiber of CNS Toxicity in Rats

Taishi Shimazaki<sup>1</sup>, Yuzo Yasui<sup>1</sup>, Kyotaka Muta<sup>1</sup>, Naohito Yamada<sup>1</sup>, Amogh Mohanty<sup>2</sup>, Saiharshith Kandalam<sup>2</sup>, Nikhil Singh<sup>2</sup>, Aashay Tinaikar<sup>2</sup>, Rohit Garg<sup>2</sup>, Tijo Thomas<sup>2</sup>, and Toshiyuki Shoda<sup>1</sup>  
 1: Toxicology Research Laboratories, Yokohama Research Center, Central Pharmaceutical Research Institute, Japan Tobacco Inc.  
 2: AIRA Matrix Private Limited

COI Disclosure Information:  
 We declare no conflicts of interest associated with this poster



## Introduction

- Assessment of changes within the central nervous system (CNS) including single cell necrosis and vacuolation of neuron/nerve fiber is a sensitive method to evaluate toxicity associated with CNS.
- A deep learning-based algorithm for anatomical subsite wise analysis of these findings is proposed for 7 cross sections (levels) of rat brain in accordance with STP position paper.

## Materials & Methods

### Tissue Preparation

Six-week-old male Sprague-Dawley (SD) rats were necropsied after a single or repeated 4-day administration of vehicles or compounds inducing CNS toxicity. Formalin-fixed brains were sectioned in 7 levels and then whole slide images (WSIs) were prepared. The WSIs of each level were divided into training sets and test sets for single cell necrosis, vacuolation of neuron/nerve fiber, and region segmentation across 7 levels of the brain.

### Training Phase with Convolutional Neural Network (CNN)

For training the deep learning models, we selected 1024x1024 size tiles at 40x magnification for single cell necrosis and vacuolation of neuron/nerve fiber, and 2048x2048 size tiles at 2.5x magnification for anatomical subsites segmentation across 7 levels of rat brain (Figure 1). The WSIs of the training sets (Table 1) were annotated with respective findings and various neuroanatomic subsites and were used to train the algorithm.

U-Net based deep learning models with variants of EfficientNet<sup>2</sup> as backbone were trained on these datasets for the segmentation of above mentioned parameters.

The network architecture for the EfficientNet-b4 model is shown in Figure 2.

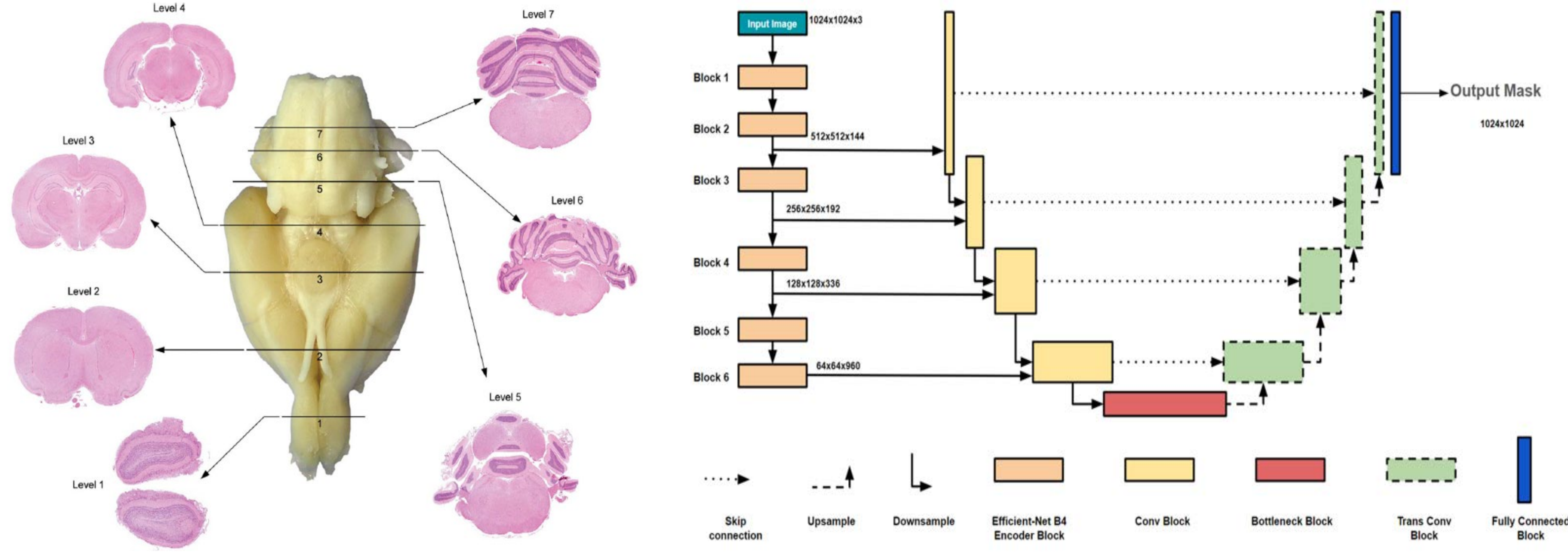


Figure 1: STP Position Paper: Recommended Practices for Sampling and Processing Brain<sup>1</sup>

Parameters	Training Dataset	Model
<b>Anatomical Subsites</b>		
Level 1	Level 1: 49 WSIs (trained with tiles of size 2048 x 2048 at 2.5x)	EfficientNet-b0
Level 2-4	Level 2-4: 99 WSIs (trained with tiles of size 2048 x 2048 at 2.5x)	
Level 5-7	Level 5-7: 99 WSIs (trained with tiles of size 2048 x 2048 at 2.5x)	
Single cell necrosis	50 WSIs (tiles of size 1024x1024 dimensions at 40x magnification)	
Vacuolation	50 WSIs (tiles of size 1024x1024 dimensions at 40x magnification)	EfficientNet-b1

Table 1: Training Dataset and Model Architecture Details

### Validation Phase

The test dataset of the brain from non-treated group (N=5/Level) and the group treated with certain compounds (N=5/Level) was analyzed to classify neuroanatomic subsites and to detect single cell necrosis and vacuolation for validation.

The classified neuroanatomic subsites by the developed model were confirmed by JSTP-certified pathologists (Figure 3).

The average of the percentage of regions where single cell necrosis was detected in the non-treated group or treated group at each level was calculated (Figure 5).

For each animal, annotation results were confirmed by the pathologist (Figure 4) and 100 neurons were counted for each level and each animal (total: 7000 cells; 100 cells x 7 levels x 10 animals), and the number of true positives (TP), false positives (FP), false negatives (FN), and true negatives (TN) were counted to generate statistical parameters indicating the performance of detection of the finding (Table 2).

### Utilization of the Model After Validation

WSIs of rat brains treated with compounds A, B and C (N=3/group) were analyzed using the model to create annotated results and quantitative values for all the levels. In addition, a blind evaluation was performed by a certified-pathologist by assessing the sections for CNS toxicological findings. Then the quantitative values from the model were compared with the pathologist's assessment outcomes (Figure 7, 9 and 11). Finally, the pathologist reviewed and confirmed the annotated results (Figure 8, 10 and 12).

## Discussion & Conclusion

- The results from the model for classifying neuroanatomic subsites and detecting single cell necrosis and vacuolation of neuron/nerve fiber at 7 levels in H&E slides correlated strongly with the pathologists' findings.
- The solution provided an automated, objective and accurate method for assessment of toxicity changes occurring in rat brain. Further, the model was able to accurately classify, detect and quantify even the very slight changes observed in each anatomical brain region at each level.
- This method can be used as an adjunctive function in pathologists' histopathological evaluation, for CNS toxicity screening in early non-GLP toxicity studies.

## Results

### Results of Classification of Neuroanatomic Subsites by the Model

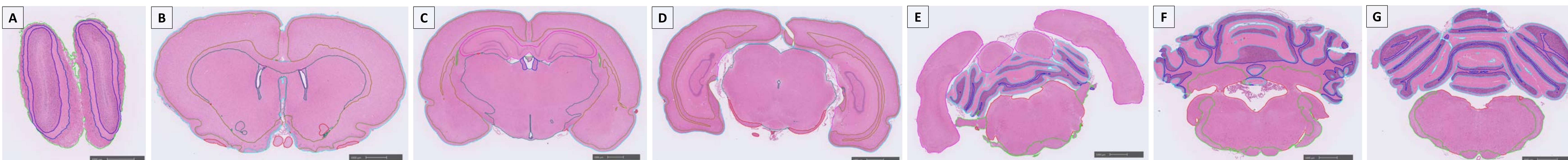


Figure 3: Classification of neuroanatomic subsites by the model

- A: Level 1**
  - Olfactory nerve layer
  - External plexiform layer
  - Granular layer
- B: Level 2**
  - Outer layer of cortex
  - Cortex
  - Caudate putamen
  - Ventricles
- C: Level 3**
  - Outer layer of cortex
  - Cortex
  - Hippocampus
  - Thalamus
  - Ventricles
- D: Level 4**
  - Outer layer of cortex
  - Cortex
  - Hippocampus
  - Brain stem
  - Outer layer of brain stem
  - Ventricles
- E: Level 5**
  - Inferior colliculus
  - Molecular layer
  - Granular layer
  - Brain stem
  - Outer layer of brain stem
  - Ventricles
- F: Level 6**
  - Molecular layer
  - Granular layer
  - Brain stem
  - Outer layer of brain stem
- G: Level 7**
  - Molecular layer
  - Granular layer
  - Brain stem
  - Outer layer of brain stem

### Results of Validation Phase of the Model (Single Cell Necrosis of Neuron)

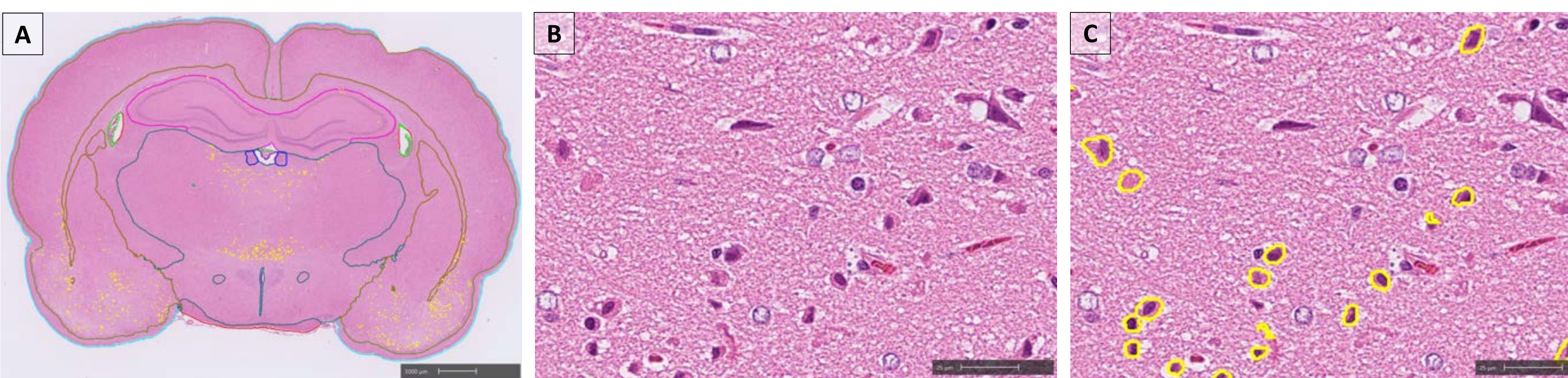


Figure 4: Detection of single cell necrosis of neuron by the model

- A:** The model was able to recognize and quantify single cell necrosis (yellow) at level 3<sup>#</sup>. (#: front-parietal cortex/auditory cortex, piriform cortex, amygdaloid nuclei, hippocampus, thalamus and hypothalamus).
- B:** High magnification of A. Slight single cell necrosis was observed at hypothalamus (without annotation)
- C:** Annotated image of B. Slight single cell necrosis was detected at hypothalamus (with annotation)

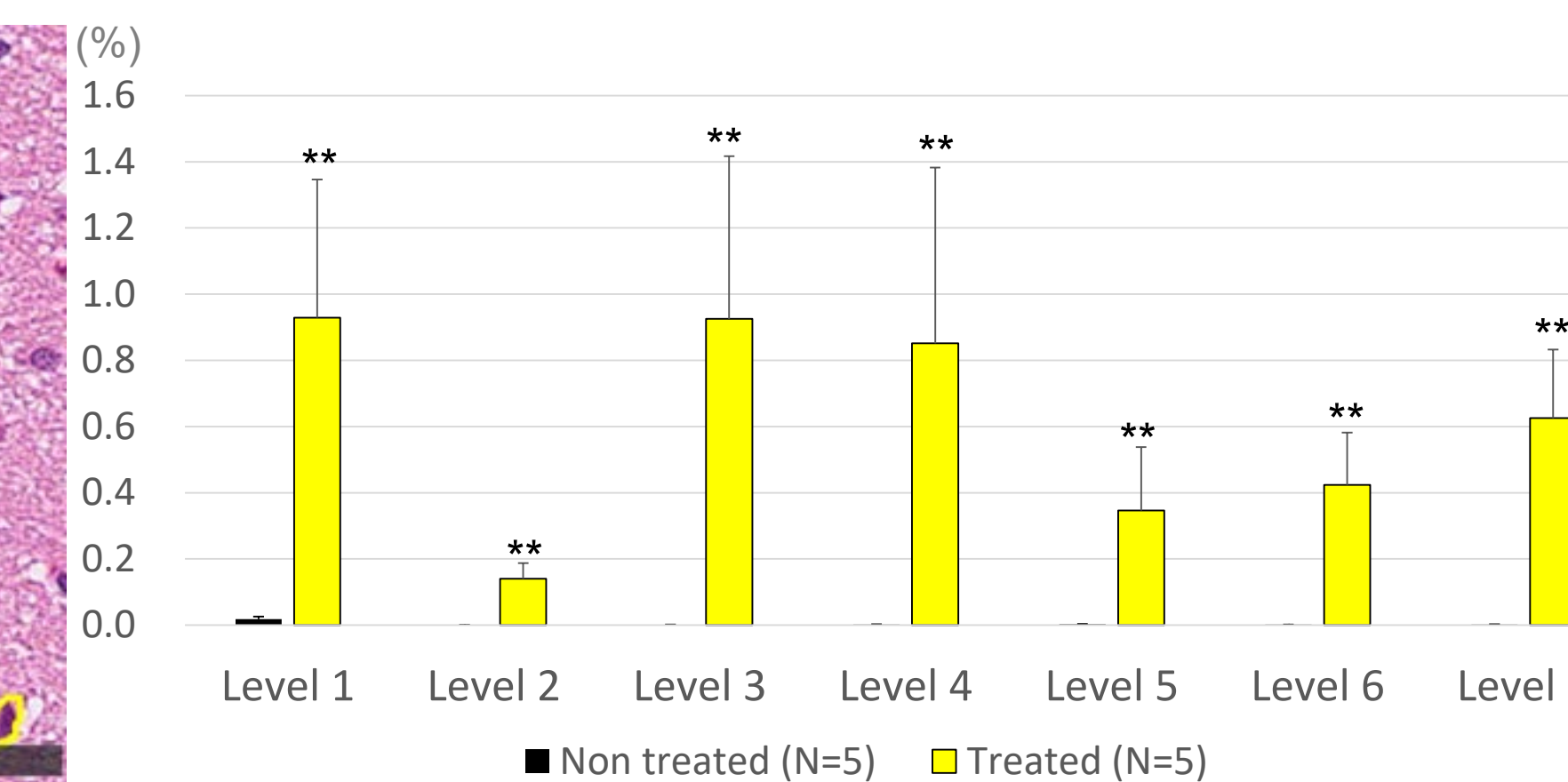


Figure 5: Comparison of the percentage of areas where single cell necrosis was detected in each level of the non-treated and treated groups. The percentage of single cell necrosis detected by the model in the non-treated group was almost zero, whereas the percentage of single cell necrosis in the treated group with test compounds was significantly increased at all the levels. \*\*, p < 0.01 (Student's t-test)

Findings	Recall	Precision	F1 Score	No. of neuron
Single cell necrosis of neuron	0.97	0.90	0.93	7000

$$\text{Recall} = \frac{TP}{TP + FN} \quad \text{Precision} = \frac{TP}{TP + FP} \quad \text{F1 Score} = \frac{2 \times \text{Precision} \times \text{Recall}}{\text{Precision} + \text{Recall}}$$

### Results of the Detection of Drug-induced CNS Toxicities Using the Model after Validation

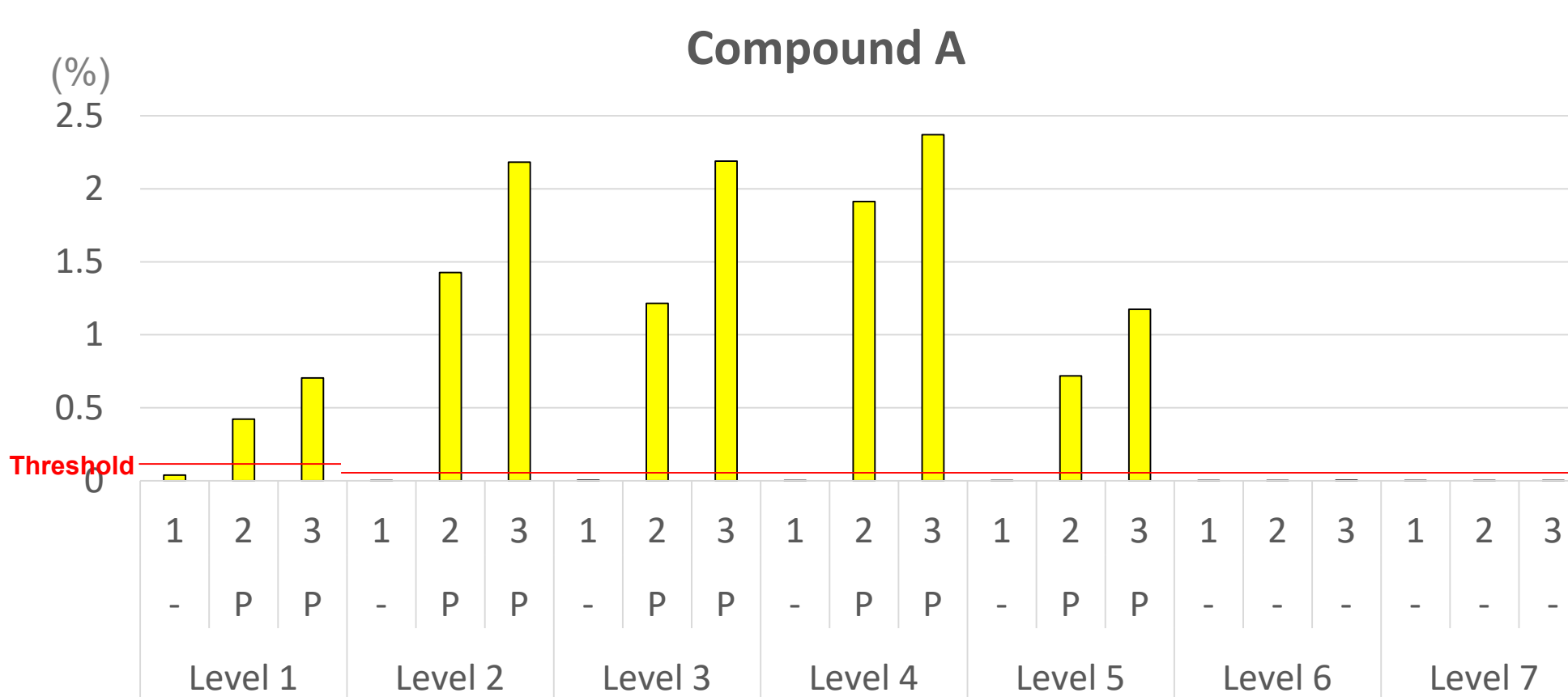


Figure 7: Percentage of single cell necrosis of neuron in each level of animals treated with Compound A (N=3/Level)

Single cell necrosis increased at Levels 1 to 5 in 2 animals (No. 2 and 3), suggesting drug-induced effects on the cerebrum or brainstem. And These quantitative values correlate with the pathologist's diagnosis.  
 -: No single cell necrosis was observed by pathologists.  
 P: Single cell necrosis was observed by pathologists.  
 Threshold: Level 1=0.05, Levels 2-7=0.03

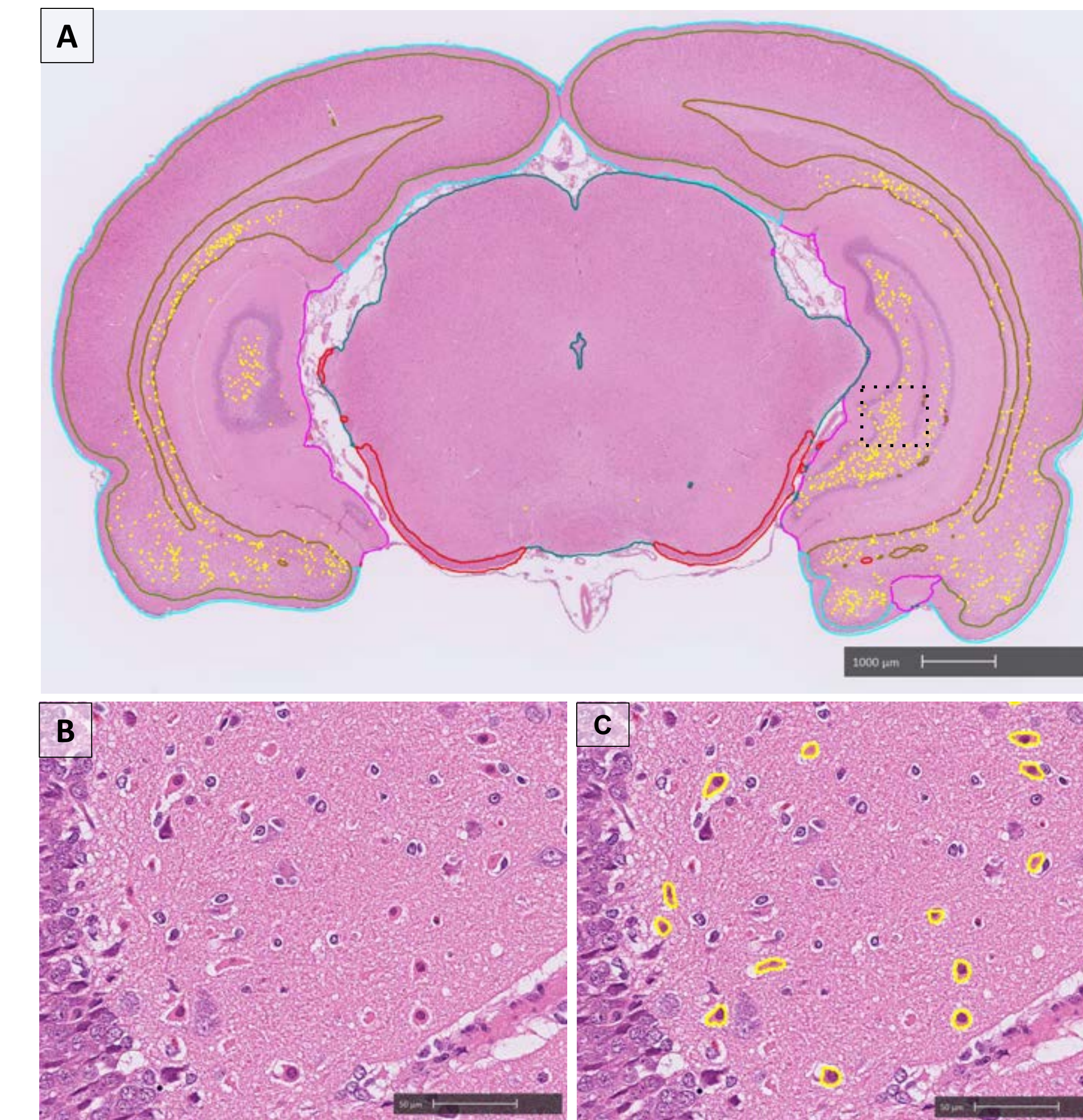


Figure 8: Detection of single cell necrosis of neuron at Level 4 in animals treated with Compound A

- A:** Single cell necrosis was detected at Level 4<sup>#</sup>. (#: auditory cortex, subiculum/ hippocampus and entorhinal cortex).
- B:** High magnification of A. Slight single cell necrosis was observed at subiculum/ hippocampus (without annotation).
- C:** Annotated image of E. Slight single cell necrosis was detected at subiculum/ hippocampus (with annotation).

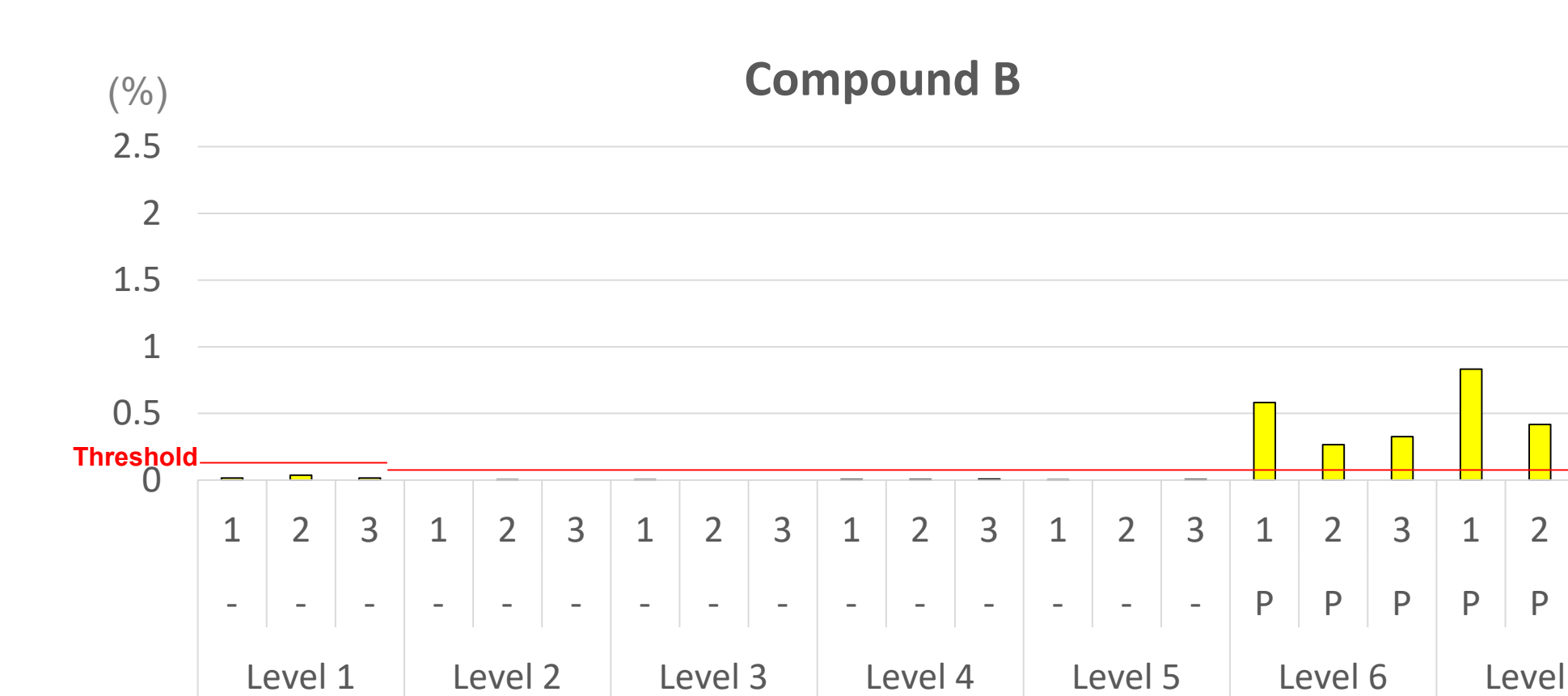


Figure 9: Percentage of single cell necrosis of neuron in each level of animals treated with Compound B (N=3/Level)

Single cell necrosis increased at Levels 6 and 7 in all animals, suggesting drug-induced effects on the cerebellum or brainstem. These quantitative values correlate with the pathologist's diagnosis.  
 -: No single cell necrosis was observed by pathologists.  
 P: Single cell necrosis was observed by pathologists.  
 Threshold: Level 1=0.05, Levels 2-7=0.03

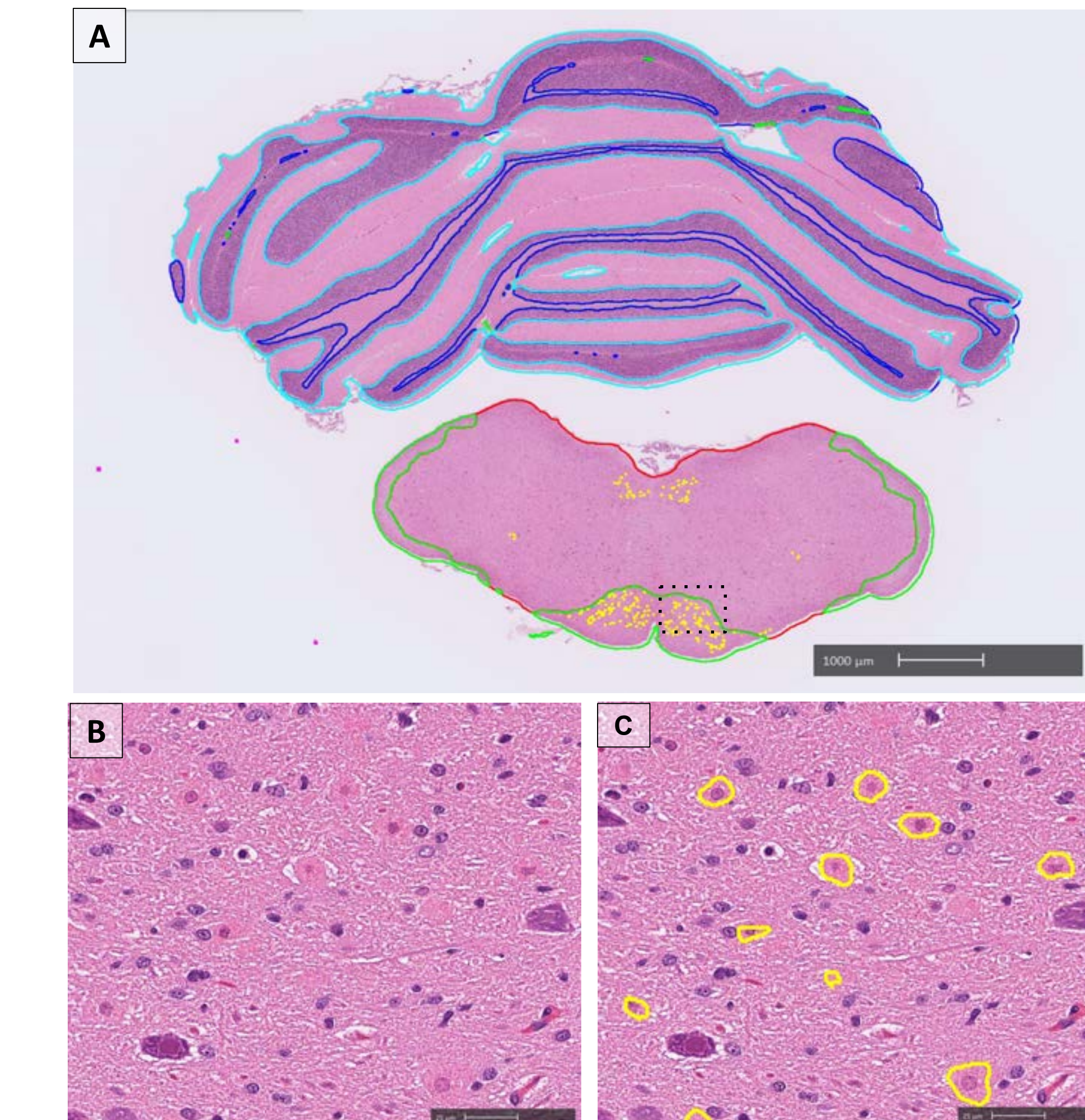


Figure 10: Detection of single cell necrosis of neuron at Level 7 in animals treated with Compound B

- A:** Single cell necrosis was detected at Level 7<sup>#</sup>. (#: hypoglossal nuclei, reticular nuclei and inferior olivary nuclei).
- B:** High magnification of A. Slight single cell necrosis was observed at inferior olivary nuclei (without annotation).
- C:** Annotated image of E. Slight single cell necrosis was detected at inferior olivary nuclei (with annotation).

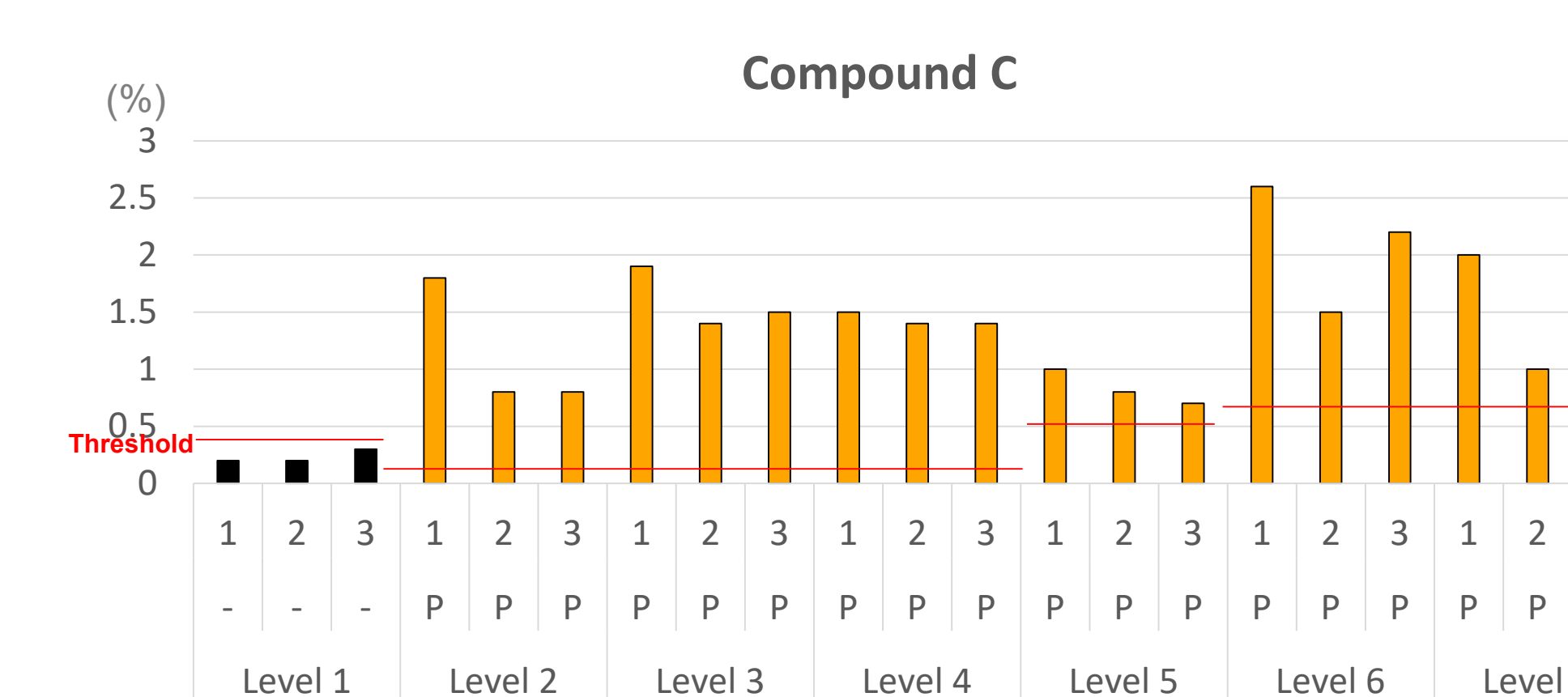


Figure 11: Percentage of vacuolation of nerve fiber in each level of animals treated with Compound C (N=3/Level)

Vacuolation increased at Levels 2 to 7 in all animals, suggesting drug-induced effects on the cerebrum, cerebellum or brainstem. These quantitative values correlate with the pathologist's diagnosis.  
 -: No vacuolation was observed by pathologists.  
 P: Vacuolation was observed by pathologists.  
 Threshold: Level 1=0.4, Levels 2-4=0.1, Levels 5=0.5, Levels 6-7=0.7

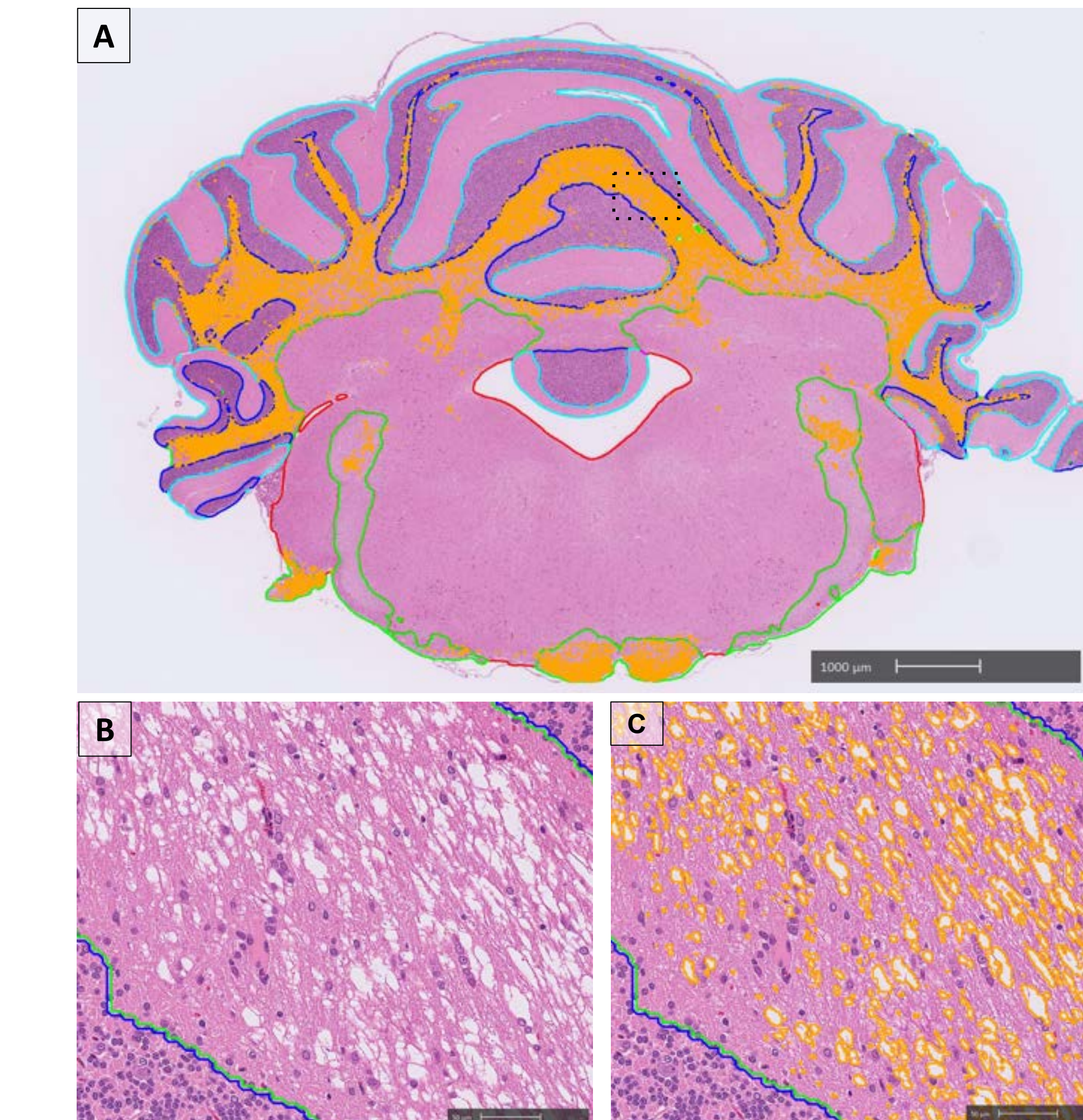


Figure 12: Detection of vacuolation of nerve fiber at Level 6 in animals treated with Compound C

- A:** Vacuolation was detected at Level 6<sup>#</sup>. (#: corpus medulla, facial nerve and trapezoid body/pyramidal tracts)
- B:** High magnification of A. Vacuolation was observed at corpus medulla (without annotation).
- C:** Annotated image of B. Vacuolation was observed at corpus medulla (with annotation).

## References

- Bolon B, Garman R, Pardo I, Jensen K, Sills R, Roulois A, Radovsky A, Bradley A, Andrews-Jones L, Butt M and Gumprecht L, *Toxicologic Pathology*, Vol 41 p.1028-1048, 2013
- Tan M, Le Q. *EfficientNet: Rethinking Model Scaling for Convolutional Neural Networks*. Proceedings of ICML, 2019